# Determining the Best Zone for Waste Storage Ponds: Integrating DEM Analysis and Satellite Gravity Data in the Prospect Area of the Ungaran Geothermal Mining Working Area, Semarang, Indonesia

**Wahyuni Annisa Humairoh[1*], Dani Mardiati [2], I Putu Raditya Ambara Putra[3]**
Departement of Geological Engineering, UPN Veteran Yogyakarta, Yogyakarta

Email: [1*]wahyuni.annisahumairoh@upnyk.ac.id, [2]dani.mardiati@upnyk.ac.id, [3]i.puturaditya@upnyk.ac.id

Received: 2025-08-26 Received in revised from 2025-09-03Accepted: 2025-09-10

***Abstract***

The Ungaran Geothermal Mining Working Area, situated on Mount Ungaran, boasts geothermal prospects in Gedongsongo and Nglimut, which can potentially expand into significant Indonesian geothermal exploration projects. The geothermal exploration industries in Indonesia face difficulties due to the PLTP industry, which generates geothermal waste in the form of geothermal mud and brine. This trash can pose a risk to ecosystems and human health if it is released into the environment. The purpose of this study was to identify the most suitable location for waste ponds in the Ungaran geothermal potential region. The method integrates data analysis of Digital Elevation Model (DEM) imagery, Landsat imagery, and air gravity data, producing integrated maps, such as Maps of Fault and Fracture density and Maps of Land Cover. Second vertical derivative (SVD) analysis from satellite gravity data is also used to ensure the presence of a structure. Five factors determine the suitability of a site for pond-making: it must be a non-residential area with a slope of less than 15%, be more than 200 meters from the fault, more than 100 meters from the road, and be more than 200 meters from locations with geothermal manifestations, such as fumaroles and hot springs. Based on the interpretation of the integrated maps resulting from the analysis, several zones in the Nglimut and Gedongsongo prospect areas are fit for constructing waste ponds. The Nglimut area has potential zones, in contrast. In the Gedongsongo area, there are no potential zones. The Nglimut prospect has two possible zones; the best zone is N2, where all five parameters are perfectly satisfied. The northern area of N1 has one geothermal manifestation (hot spring). The best-to-fair zones are N2 and N1.

***Keywords:*** *Digital Elevation Model; Landsat Imagery; Nglimut; Second Vertical Derivative, Ungaran*

## 1. Introduction

Geothermal energy in Indonesia holds enormous potential. The country has the most extensive geothermal reserves in the world, due to its position on the “Ring of Fire,” and volcanic activity provides an abundance of geothermal resources. However, while geothermal energy is often promoted as a clean and renewable energy source, environmental concerns related to waste and byproducts must be carefully considered. Geothermal developers in Indonesia tend to focus too much on rig equipment and well construction when planning drilling operations, often oversimplifying matters related to drilling waste. This, in fact, often leads to negative impacts on the overall drilling project, where poor waste management creates environmental pollution that harms the local community [1].

In Indonesia, geothermal drilling and operations generate various types of waste, which are regulated under Government Regulation No. 101 of 2014 on the Management of Hazardous and Toxic Waste. These wastes are classified into domestic waste (solid and liquid), non-B3 waste, and B3 (toxic and hazardous) waste [1]. Within the geothermal power plant (PLTP) sector, exploration and production activities generate significant amounts of brine and drilling mud. Studies show that these byproducts often contain toxic substances such as arsenic, mercury, boron, and antimony, which can precipitate as the fluid cools [3]. If discharged without treatment, geothermal brine and mud can contaminate soil and groundwater, reduce water quality, and disrupt aquatic ecosystems, while also posing long-term health risks to humans and animals [4], [5]. To avoid leaks that could pollute the environment, the maintenance pond should be situated in an area with flat, stable topography and minor geological structure. Geothermal power plants, including waste ponds, are located based on five criteria (**Table 1**): non-residential land cover areas, a slope of less than 15%, a distance of more than 200 meters from the fault, a distance of more than 100 meters from the road, and a distance of more than 200 meters from areas of geothermal manifestations, such as fumaroles and hot springs [6], [7], [8].

**Table 1. Geothermal power plant location determination parameters** [6]

| Parameters | Unmatched area for geothermal power plants and waste ponds |
|---|---|
| Land Cover Area | Residential area |
| Land Slope | Area with a slope of more than 15% |
| Fault Zone | Fault zone with a buffer of 200 m |
| Road Access | Road access with a buffer of 100 m |
| Geothermal Manifestation Locations | Geothermal Manifestation with a buffer of 200 m |

Geothermal energy in the Mount Ungaran area has great potential in the Nglimut and Gedongsongo area (see **Figure 1**). Two prospect locations with a combined geothermal energy potential of 110 MWe have been identified by the Center for Geological Resources (PSDG) in the Ungaran Geothermal Mining Working Area [9]. This study aims to specify the most suitable zone for waste ponds in the Ungaran geothermal prospect area.

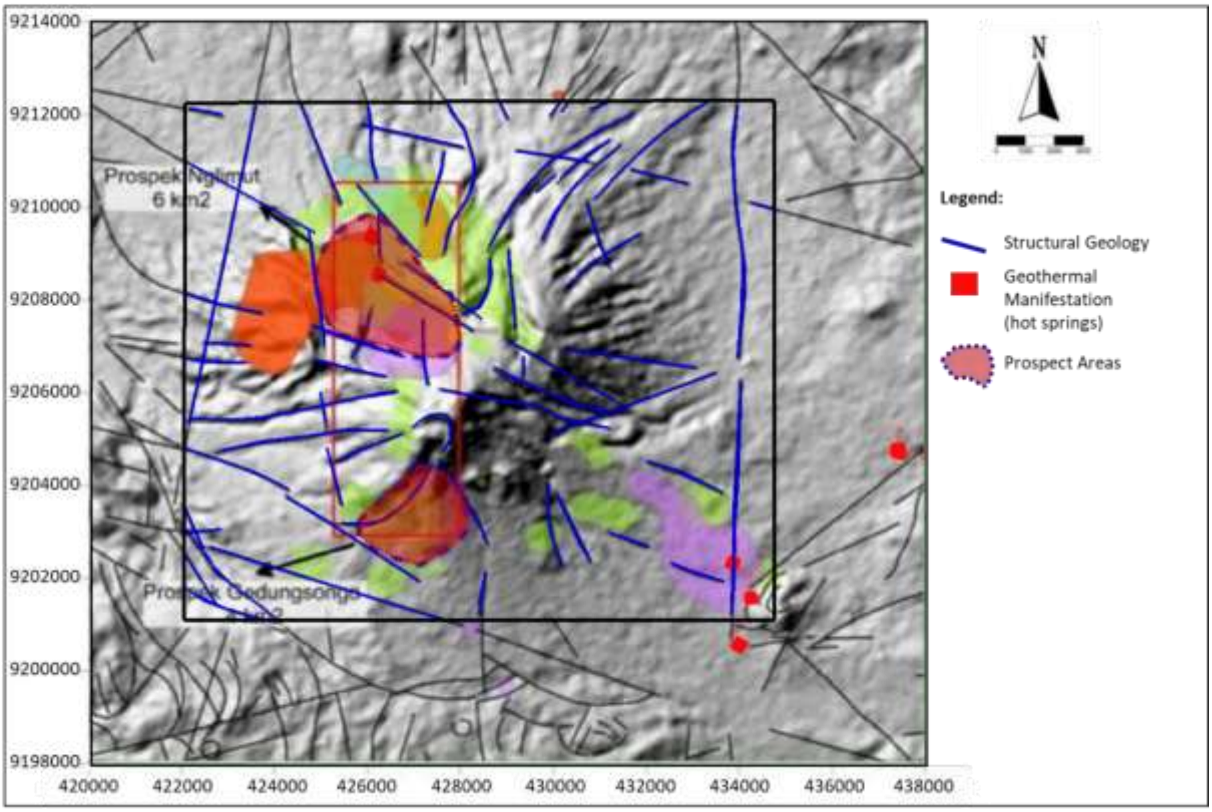


**Figure 1. The Nglimut and the Gedongsongo geothermal prospect.** [2].

## 2. Method

This study utilized Digital Elevation Model (DEM) data for Mount Ungaran to extract slope and lineament information, acquired from the Geospatial Information Agency (BIG). Additionally, patterns of land cover in the study area were examined using Landsat images from the United States Geological Survey (USGS). The research was conducted in the Ungaran Geothermal Mining Working Area, Central Java, which spans 298 km² between 7°08′–7°16′ S and 110°19′–111°29′ E, as defined by the Minister of Energy and Mineral Resources' Decree No. 1789K/33/MEM/2007. According to Zhou and Liu [10], DEMs provide a digital representation of the Earth's surface, enabling the determination of topographical factors such as elevation, slope, aspect, and watershed boundaries. Landsat has been providing multispectral imagery for land monitoring from its initial launch in 1972 under the moniker ERTS-1 (Earth Resources Technology Satellite-1) and its subsequent renaming as Landsat-1. The program has since advanced to Landsat-9, with enhanced spectral capabilities across different electromagnetic ranges [11]. By combining the analysis of DEM and Landsat imagery, the technique creates maps of land cover, fault and fracture density, and integrated slope and lineament using ArcGIS 10.3.

Furthermore, analyzed gravity field anomalies using gravity disturbance data from the Global Gravity Model Plus, commonly referred to as GGMPlus2013 [12]. GGMPlus combines GRACE, GOCE gravity satellite data, and the Earth Gravity Model (EGM, 2008) [13]. The resolution of the grid data from GGMPlus is quite good, as it has a grid spacing of 200m. The topographic correction was then performed using Python's Harmonica module/library (Fatiando a Terra Project, 2023). The method used was forward modeling of the topographic masses with a rectangular prism mesh shape. The surface elevation data used were Global Bathymetry and Topography, SRTM15+ [14], downloaded using the PyGMT module [15]. The density value used is 2670 kg/m³, which is the average density of the Earth's crust. The final result obtained from this correction is equivalent to the Complete Bouguer Anomaly, as it removes the effects of surface topography. We also conducted a second vertical derivative (SVD) analysis of the topographic correction results. The SVD analysis aims to identify anomalous contrasts that may indicate the presence of a structure. The SVD calculation was performed using the vertical derivative filter module in the Harmonica Python library.

## 3. Results and Discussion

### *3.1. Maps of Slope and Lineaments*

Digital Elevation Model (DEM) analysis was used to generate slope and lineament maps of the study area (**Figures 2** and **3**). The slope map was divided into two classes: areas with slopes less than 15% were shown in green, while areas with slopes greater than 15% were shown in red [2]. The classification threshold of 15% slope was adopted following [6], [7], [8], who identify zones with slopes below this value as suitable locations for pond construction.

The slope parameters are the most influential factor in landslides; the greater the slope value, the greater the potential for landslides [16]. The slope value ranges from 14% to 20%, described as moderately steep, and values above those are categorized as steep slopes. This correlates with one of the parameters for the geothermal power plant and waste pond locations (**Table 1**).

A Digital Elevation Model (DEM) and geological structure data were utilized to process the lineament map, as quantitative geomorphology is a key focus in this research area [9]. The tectonic activity led to the development of various geological structures [17]. The formed structural patterns reflect the dominant stress patterns resulting from specific tectonic processes with varying orientations in the lineament map, as determined using DEM data. The resulting stress patterns give rise to structures such as faults, fractures, and folds at various scales, ranging from regional to local.

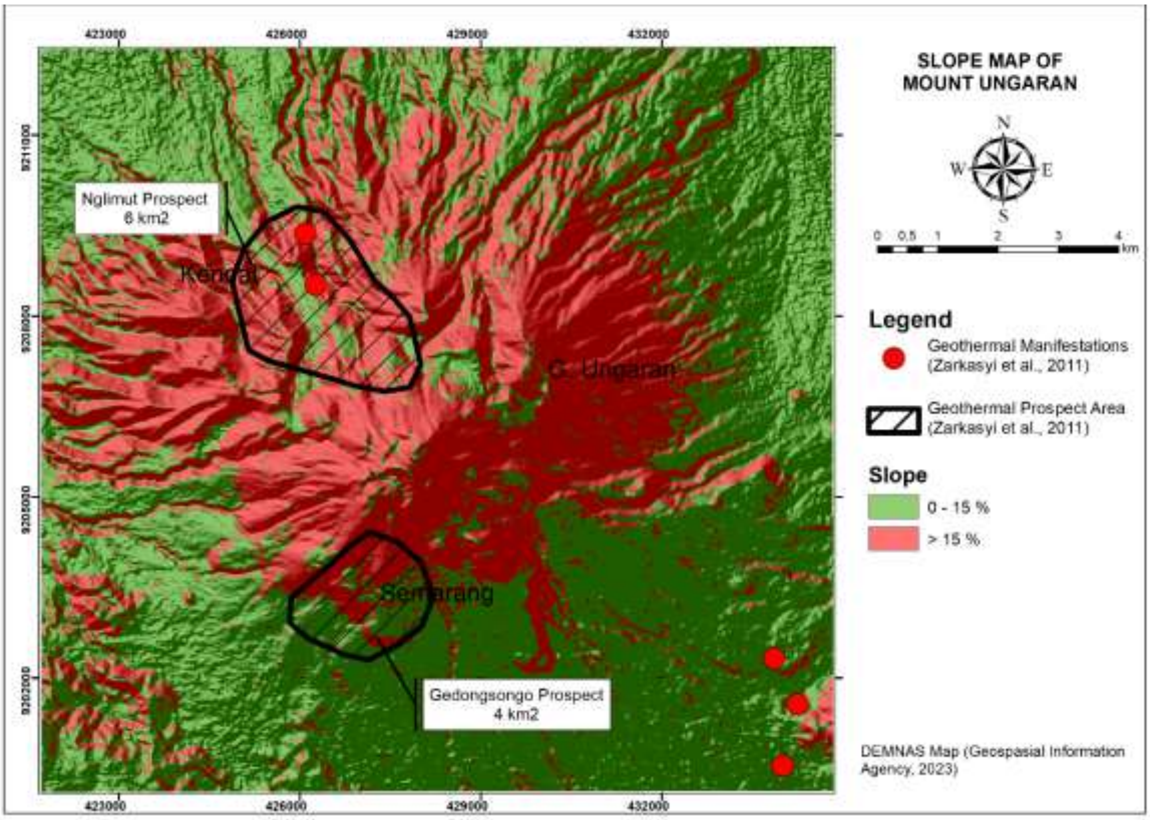


**Figure 2. A map of the slope showing the green field that can be used to create ponds with a slope of less than 15%** [2]

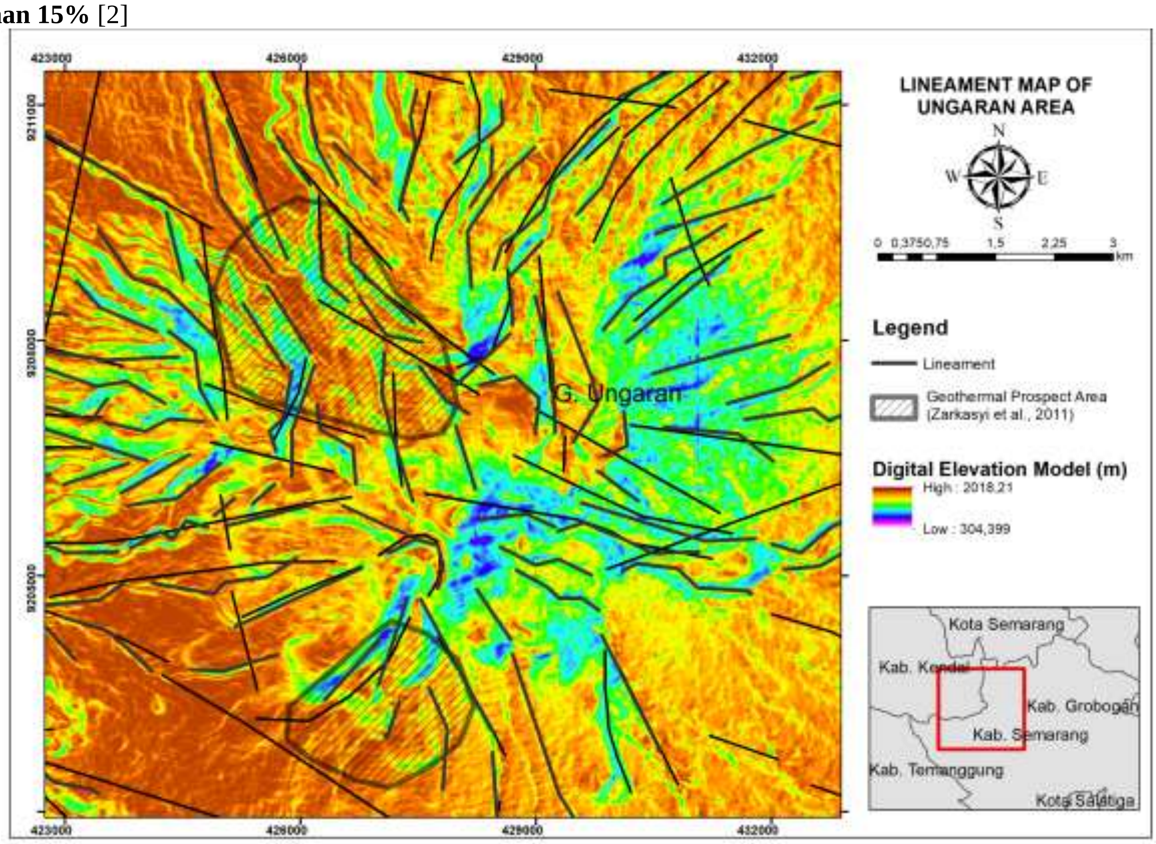


**Figure 3. A lineaments map that incorporates extra details from regarding the geological structure, prospect areas, and manifestation spots** [9].

The presence of geological structures and lineaments in the research area is depicted on this map. The map contrast that aids in identifying lineaments and geological features is that light regions denote high areas and dark areas denote low areas. The lineament map generated from DEM analysis serves as an essential dataset for developing fault and fracture density maps. Lineaments are surface expressions of underlying structural features such as faults, joints, and fractures, which play a key role in controlling fluid pathways within geothermal systems. Mapping their orientation and density allows the identification of structurally controlled zones that may enhance hydrothermal circulation and permeability [18]. Fault and fracture density maps derived from lineament analysis have been widely applied in geothermal exploration to delineate favorable reservoir zones and target areas for further investigation. Thus, the lineament map constitutes a critical input for understanding subsurface structural frameworks. Data extraction is performed on the topographic map of the research area by drawing lines [17].

### *3.2. Maps of Fault and Fracture Density*

Lineament maps serve as input data for generating Fault and Fracture Density (FFD) maps. FFD maps calculate a magnitude per unit area based on lineaments within a specified radius around each cell. There are two criteria for a likely pond-making and PLTP site: The span from faults or fractures must be greater than 200 meters, and the length from locations of geothermal manifestations must be greater than 200 meters [6]. FFD will divide the area from the most fault-influenced to the least fault-influenced (0 per square kilometer).

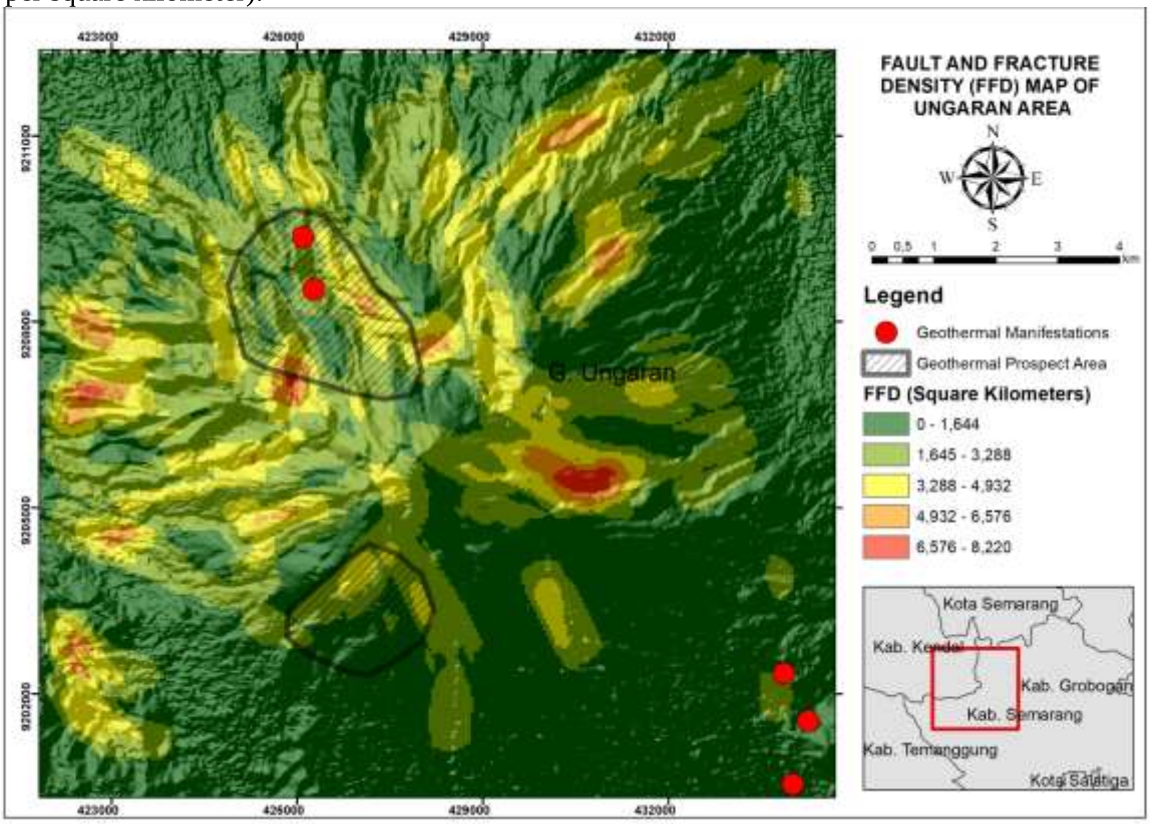


**Figure 4. The Fault and Fracture Density maps of the research area. Green and light green colors represent the area with stable conditions. That area has a negligible impact on existing faults or fractures**

The Fault and Fracture Density map (**Figure 4**) is calculated from lineament interpretation. Based on the FFD maps, the area is divided into five categories based on FFD value per square kilometer. (see Figure 4) green (0 – 0.84 km-1), light green (0.84 – 1.68 km-1), yellow (1.68 – 2.53 km-1), orange (2.53 – 3.37 km-1), and red (3.37 – 4.22 km-1) zones. The stable area with the least minor fault/fracture influence is the green and light green zone (0 – 1.68 km-1).

### *3.3. Map of Land Cover*

Landsat image data were processed to create a land-cover map of the research area (**Figure 5**). Nine regions were identified on this map: brushwood, paddy fields, open land uses, dryland and mixed dryland agriculture, brushwood, secondary dryland forest, plantation forest, and residential plantations. Based on the parameters for determining the location of ponds [6], residential areas, indicated by dark brown, should be avoided.

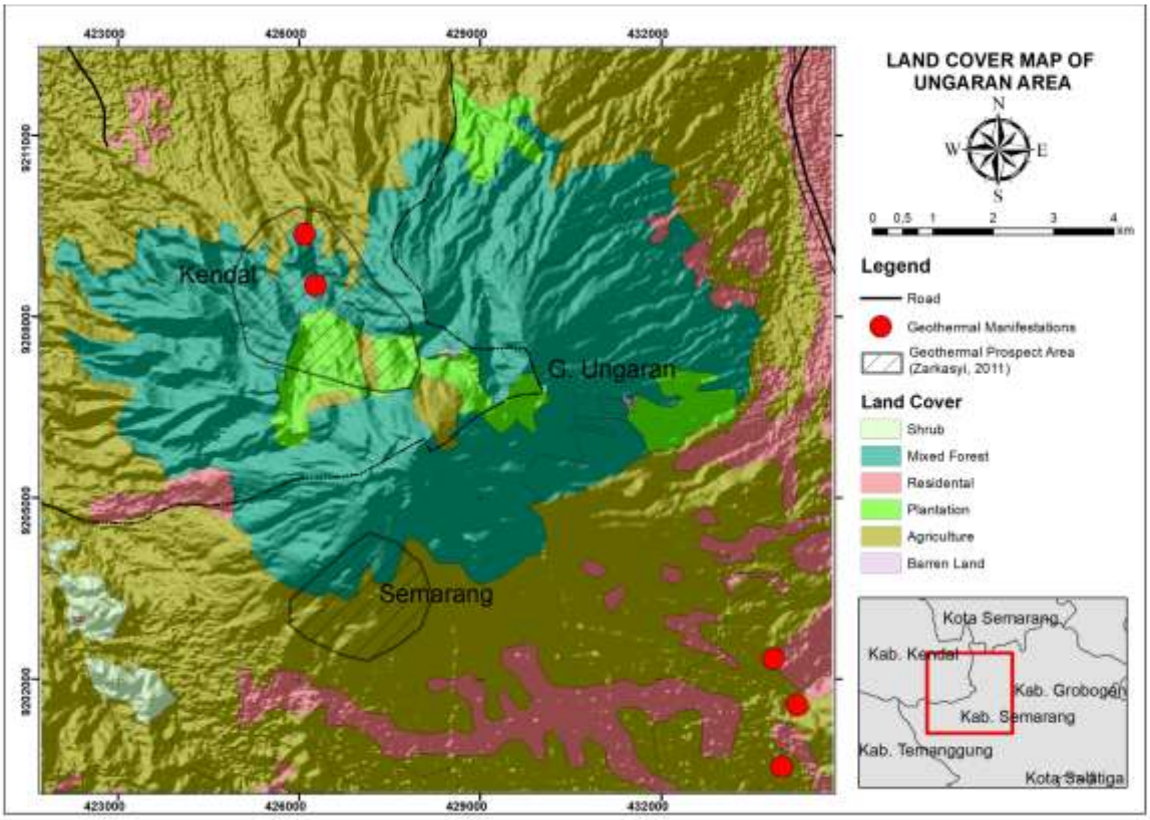


**Figure 5. The Land Cover Map was divided into nine regions: brushwood, secondary dryland forest, plantation forest, residential areas, dryland agriculture, mixed dryland agriculture, paddy fields, and open land**

### *3.4. Second Vertical Derivative*

Structural analysis in the Ungaran Geothermal Working Area was conducted using a combination of Digital Elevation Model (DEM)–derived lineament mapping and gravity data interpretation through second vertical derivative (SVD) analysis. The lineament map, produced using DEM data, displays the surface expressions of structural elements, such as fractures and faults. These lineaments were further quantified to develop fault and fracture density maps, which highlight zones of structurally controlled permeability that are favorable for hydrothermal circulation [4][18]. High lineament density zones are interpreted as potential fluid pathways, making them critical indicators for geothermal exploration, but they must be avoided in areas designated for waste storage ponds.

The Bouguer anomaly data are the input for generating SVD maps (**Figure 7**). SVD enhances short-wavelength anomalies associated with shallow density contrasts while suppressing regional trends, thus allowing for the precise delineation of faults, fractures, and lithological contacts that may not be evident in Bouguer anomaly maps (**Figure 6**). In the Ungaran geothermal area, the SVD map reveals anomalous linear features that correspond to probable fault zones, which are consistent with lineament density patterns derived from DEM interpretation. Although prior to the data resolution, satellite gravity data cannot clearly specify the detailed fault occurring in the study area for the SVD map.

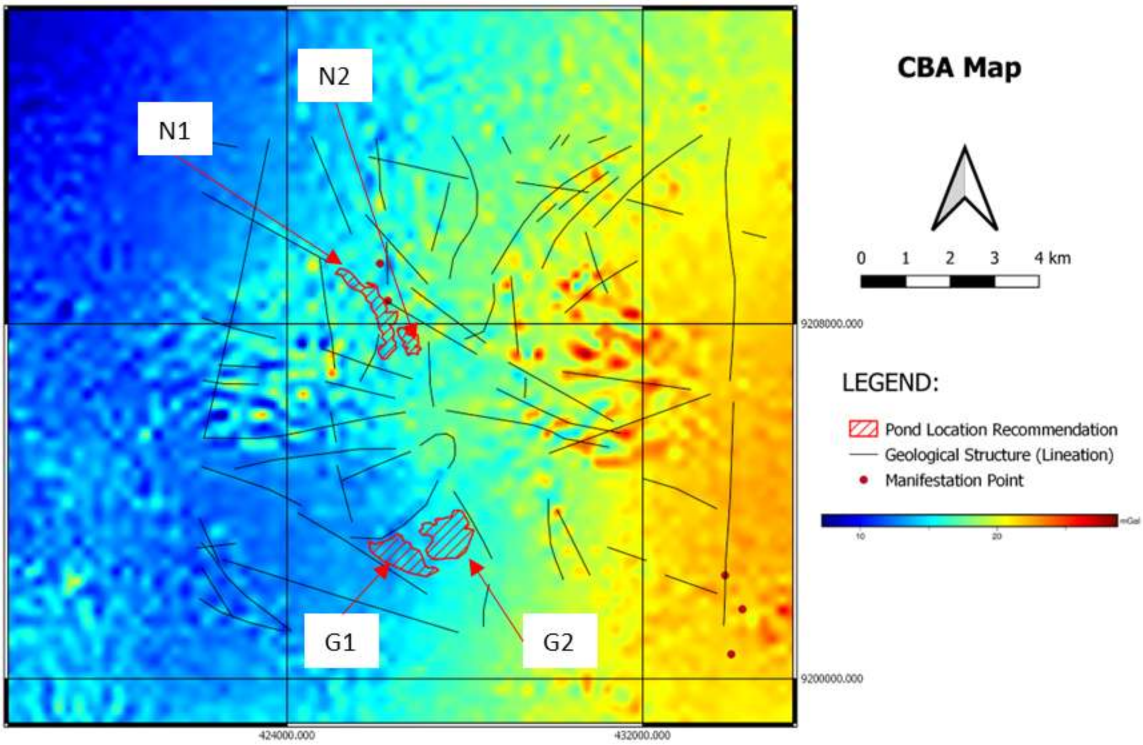


**Figure 6. Map of Complete Bouguer Anomaly with potential wasted pond area from the previous study [2], two delinations for Nglimut and two delinations for Gedongsongo**

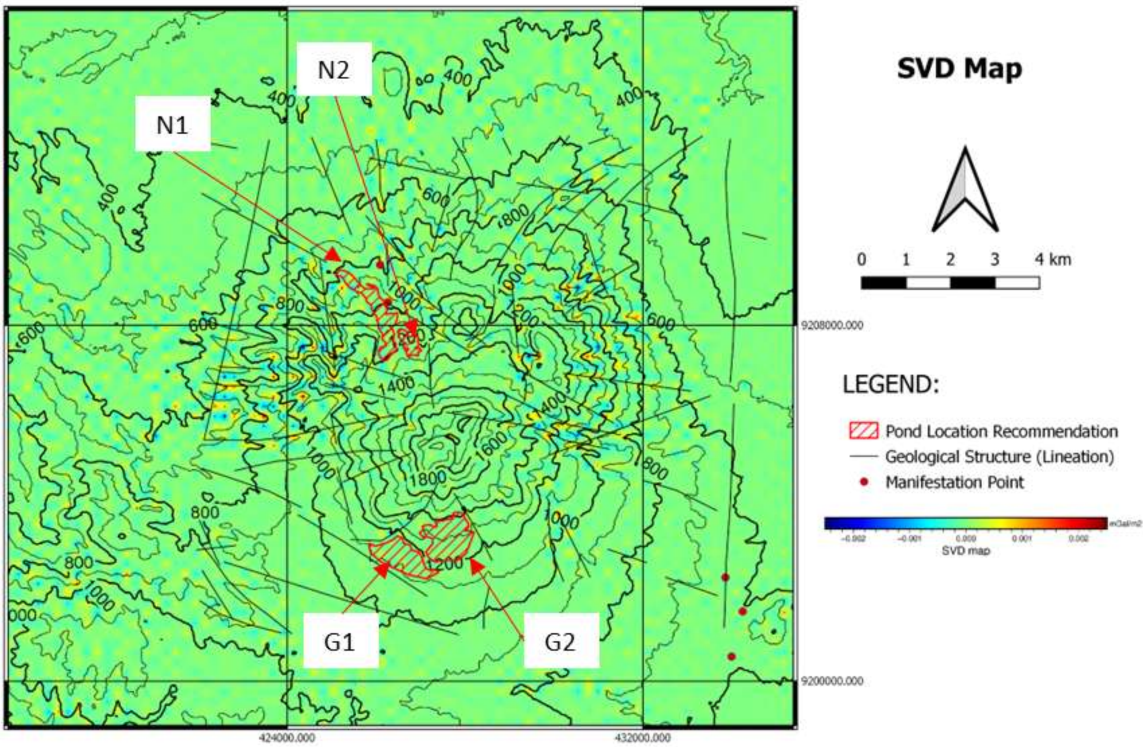


**Figure 7. Second Vertical Derivative Analysis with potential wasted pond area from the previous study [2], two delinations for Nglimut and two delinations for Gedongsongo**

The selection of suitable sites for constructing waste storage ponds was concentrated in the Nglimut and Gedongsongo prospect areas, as both are considered potential locations for future PLTP development. The identification of the optimal pond site was guided by five key criteria: land cover, slope conditions, proximity to fault structures, accessibility via existing roads, and distance from geothermal source locations.

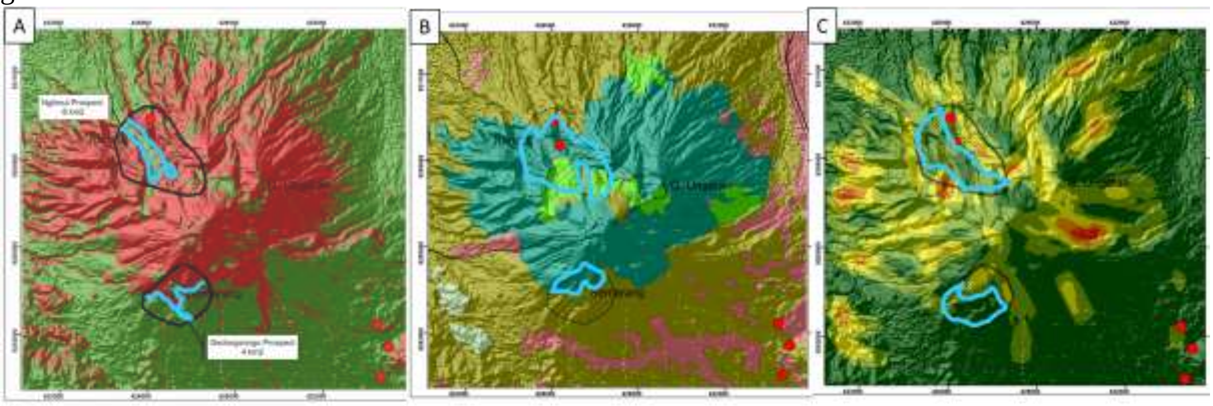


**Figure 8. Delineation results indicate the best area, as indicated by the blue line, for the waste storage pond, as shown in three maps: A. Slope Map, B. Land Cover Map, and C. Fault and Fracture Density Map**

The best fit for the wasted storage pond area from the Slope maps is with a slope less than 15% [2], [6], [7], [8], as indicated by the green color in the map. In the Land cover map, residential areas, shown in dark brown, must be avoided. Quantitative geomorphology is employed to determine the presence of tectonic activity based on calculations of morphological values [17]. In this study, that information is depicted in the Fault and Fractures Density Map (FFD), where the stable area with the least minor fault/fracture influence is represented by the green and light green zones (0 – 1.68 km-1). Based on the overlay results of the Map of Slope, Fault and Fracture Density (FFD) Map, and Land Cover Map, with supporting information from the SVD Map (**Figure 8**), there are no potential pond zones in the Gedongsongo prospect. Additionally, the NW-SE-oriented geological structure is flattened by the right-slip fault, which is the fracture aquifer system on the southern slope of Mount Ungaran, as observed at the Gedongsongo prospect [19]. This condition reinforces the unsuitability of the area around the Gedongsongo prospect as a location for making a waste pond.

Among the two evaluated sites, the Nglimut and Gedongsongo prospects, only the Nglimut prospect satisfies all five criteria used to determine suitable locations for geothermal waste disposal ponds, namely land cover, slope, proximity to faults, road accessibility, and distance from the geothermal source. This finding underscores the suitability of Nglimut as the primary candidate for waste management infrastructure to support future PLTP development. Moreover, the spatial correlation of the identified location in Nglimut with the N1 and N2 zones further strengthens the validity of this result, indicating consistency with previous structural and geothermal assessments in the area [2].

## 4. Conclussion

The integrated analysis of DEM imagery and Landsat data, with validation using SVD data, enables the identification of optimal locations for pond construction in geothermal exploration. By combining slope maps, fault and fracture density maps, and land cover maps, surface structures and landforms suitable for pond placement can be delineated in detail, based on five key parameters. The recommended sites derived from this analysis were located outside residential areas, had slopes of less than 15%, were situated more than 200 m from faults, more than 100 m from roads, and at least 200 m away from geothermal features like fumaroles and hot springs.

From the two possible zones in the Nglimut prospect, the potentially suitable zone is N2, where the five parameters were perfectly satisfied. However, actual suitability requires field validation, such as geotechnical drilling, hydrogeological testing, and environmental impact studies. The northern area of N1 has one geothermal manifestation (hot spring). The best-to-fair zones are N2 and N1.

## Reference


[1] R. Ratna et al., "Geothermal Drilling Waste Management in Indonesia: Regulation, Practices, and Utilization", *Proceedings, 48th Workshop on Geothermal Reservoir Engineering*, Stanford, California, Feb 2023, Paper: SGP-TR-224.

[2] D. Mardiati, W. A. Humairoh, and I. P. R. A. Putra, "Preliminary study of waste storage ponds delineation area in the Ungaran Geothermal Mining working area, Semarang, Indonesia", *The 6th International Conference on Earth Science, Mineral, and Energy. IOP Conf. Series: Earth and Environmental Science,* 2024, doi:10.1088/1755-1315/1339/1/012009.

[3] M. Mukti, B. Tomaszewska, M. Starczewska, and E. O. Ningrum, "Geological and environmental implications of utilizing geothermal energy in the Lahendong working area, Indonesia", *Geology, Geophysics and Environment, Wydawnictwa AGH*, vol 48(1), pp 69–82, April 2022, doi: https://doi.org/10.7494/geol.2022.48.1.69.

[4] Hariyadi, "Wetland system for geothermal wastewater management: A case study in Lahendong, North Sulawesi", *International Research Journal of Engineering, IT & Scientific Research*, vol 8(5), pp 197-209, Sept 2022, doi: https://doi.org/10.21744/irjeis.v8n5.2181.

[5] A. Utami et al., "Geothermal energy solid waste management: Source, type of waste, and management". *2nd International Conference on Earth Science, Mineral, and Energy, AIP Conference Proceedings*, 2020, doi: https://doi.org/10.1063/5.0007299.

[6] T. Hariyanto and F. N. Robawa, "Identifikasi Potensi Panas Bumi Menggunakan Landsat 8 Serta Penentuan Lokasi Pembangkit Listrik Tenaga Panas Bumi: Kawasan Gunung Lawu", *GEOID*, vol. 12, pp 36-42, 2016.

[7] I. F. Robbany, A. Kurniawan, and M. Taufik, "Determination of Geothermal Power Plant Site from Geological Data and Digital Elevation Models", *34th Asian Conference on Remote Sensing 2013,* Bali, Indonesia, Oct 2013, Paper: P-S04-025.

[8] H. Yousefi, S. Ehara, and Y. Noorollahi, "Geothermal Potential Site Selection Using GIS in Iran", *Proceedings, Thirty-Second Workshop on Geothermal Reservoir Engineering*, Stanford, California, Jan 2007, Paper: SGP-TR-183.

[9] A. Zakarsyi, Y. Rezky, and M. Nurhadi, "Keprospekan Panss Bumi Gunung Ungaran Berdasarkan Analisis Geosain Terpadu". *Buletin Sumber Daya Geologi,* vol. 6(3), pp 111-122. 2011.

[10] Q. Zhou and X. Liu, "Error Analysis of Grid-Based Slope and Aspect Algorithms", *Photogrammetric Engineering and Remote Sensing*, vol 7(8), pp 957–962, August 2004.

[11] J. G. Masek et al., "Landsat 9: Empowering Open Science and Applications through Continuity". *Journal Remote Sensing of Environment* 248, 2020, doi: https://doi.org/10.1016/j.rse.2020.111968.

[12] C. Hirt, S. Claessens, T. Fecher, M. Kuhn, R. Pail, and M. Rexer, "New ultrahigh-resolution picture of Earth's gravity field", *Geophysical Research Letters*, vol 40(16), pp 4279–4283, 2013, doi: https://doi.org/10.1002/grl.5083.

[13] N. K. Pavlis, S. A. Holmes, S. C. Kenyon, and J. K. Factor, "The development and evaluation of the Earth Gravitational Model 2008 (EGM2008)". *Journal of Geophysical Research: Solid Earth*, vol 117(B4), 2012, doi: https://doi.org/10.1029/2011JB008916.

[14] B. Tozer, D. T. Sandwell, W. H. F. Smith, C. Olson, J. R. Beale, and P. Wessel, "Global Bathymetry and Topography at 15 Arc Sec: SRTM15+". *Earth and Space Science*, vol 6(10), pp 1847–1864, 2019, doi: https://doi.org/10.1029/2019EA000658.

[15] L. Uieda, V. Oliveira, and V. Barbosa, "Modeling the Earth with Fatiando a Terra", *Proceedings of The 12th Python In Science Conference (SCIPY 2013)*, pp 92–98, 2013, doi: https://doi.org/10.25080/Majora-8b375195-010.

[16] W. L. Turnip and S. N. Jati, "Analysis of Landslide Prone Areas in Tampahan, Toba Samosir Regency, North Sumatra Province", *JEMT*, vol 1(1), pp 25–30, 2020, doi:10.31284/j.jemt.2020.v1i1.1149.

[17] H. L. Sunan, M. Nurlatifah, F. X. A. T. Laksono, and A. Widagdo, "Analysis of tectonic influence on morphological formation: Case study of Gapura Pemalang Area". *JEMT*, vol 3(2), pp 104–123, 2023.

[18] K. Koike, S. Nagano, and M. Ohmi, "Lineament analysis of satellite images using a Segment Tracing Algorithm (STA)", *Computers & Geosciences*, vol 21(9), pp 1091–1104, 1995.

[19] N. K. Hisan, L. D. Jasaputra, P. A. Bernaldo, N. A. Y. P. Karlina, and A. Arhananta, "Hydrostructure of Groundwater Manifestation of Gedongsongo Geothermal Ungaran, Semarang, Central Java", *JEMT*, vol 1(1), pp 31–39, 2020, doi: DOI: 10.31284/j.jemt.2020.v1i1.1150.